

RELATIVISTIC PHENOMENA IN ACTIVE GALACTIC NUCLEI

M.H. Cohen¹, M.L. Lister² and R.C. Vermeulen³

Abstract. The idea that the radio jets in AGN contain material in relativistic motion is supported by many lines of observational evidence, including morphology, brightness temperature estimated with interferometers and with intrinsic variations, interstellar scintillations, X-rays, and superluminal motion. These are largely independent, and taken together make an irrefutable case for relativistic motion.

1 Introduction

Scientists were surprised in the early 1950s, when it became clear that the “radio stars” in fact were extragalactic and hence very energetic, and the general idea of a calm orderly Universe had to be questioned. In later years the discovery of black holes, quasars, pulsars, and other exotic objects changed the view completely, and brought us to the *violent* Universe as we understand it today.

In a prescient article, Rees (1966) suggested bulk relativistic motion as an explanation for the rapid variations in flux density seen in quasars; and he also predicted the phenomenon of superluminal apparent transverse velocity, which was discovered five years later. At that point most people believed that cosmic jets contained relativistic jets of plasma, but what process could collimate and accelerate whole solar masses of material to relativistic speeds? The current paradigm is that a giant black hole lies at the center of a galaxy, and the process of accretion combined with a magnetic field generates the bulk relativistic flow. The details of this scenario are not well understood, but gravitational accretion is the only known means for generating the required energy per unit volume.

In this paper we review the radio observations that provide evidence for relativistic motion. The plan of the paper is to successively discuss frequency shift, morphology and Doppler boosting, brightness temperature measured with interferometers and estimated with intrinsic variability, interstellar scintillations, inverse-Compton X-rays, and superluminal motion. Individually, and especially taken

¹ California Institute of Technology, Pasadena, CA, 91125

² Department of Physics, Purdue University, West Lafayette, IN 47907

³ ASTRON, P.O. Box 2, 7990 AA Dwingeloo, The Netherlands

together, these make a convincing case for relativistic motion in the radio jets. This conclusion is independent of any specific cosmology.

Relativistic motion implies that the observed radiation patterns are narrow, that Doppler boosting increases the observed flux density, and that the observed time scale is shrunk below that in the frame of the AGN. These affect the observable quantities; namely, frequency, luminosity, apparent transverse speed, and variability; and there should be statistical relations among them. We briefly touch on this in §4.

A number of earlier papers have discussed the different types of observational data bearing on relativistic motion. We mention only a few of them here: Ghisellini *et al.* (1993) compared X-ray and VLBI data to derive Doppler factors and compared them with other beaming indicators; Vermeulen and Cohen (1994) assembled all the existing data on superluminal sources and analyzed several models involving the distributions of Lorentz factor and of the ratio of pattern to beam velocity; Lister and Marscher (1997) made Monte Carlo calculations of distributions of the measurable parameters, and of their correlations; and Lähteenmäki & Valtaoja (1999) estimated Lorentz factors and also the intrinsic temperature in the synchrotron sources. These past surveys mainly used inhomogeneous data culled from the literature. However, two large surveys on the VLBA, at 5 MHz (Vermeulen *et al.* 2003) and 15 GHz (Kellermann *et al.* 2004, hereafter K04) are now bearing fruit, and analyses with these superior data sets should soon give much better results.

2 Formulae

Here we list some formulae, for later convenience. Assume a relativistic luminous plasma blob with velocity $\beta = v/c$ and Lorentz factor $\gamma = (1 - \beta^2)^{-\frac{1}{2}}$. If it is moving at angle θ to the line-of-sight (LOS) then its Doppler factor is

$$\delta = \frac{1}{\gamma(1 - \beta \cos \theta)} \quad (1)$$

The observed frequency is $\nu = \delta \nu^*$, where the superscript * refers to the coordinate frame of the moving plasma. Non-starred quantities are in the frame comoving with the AGN. The brightness temperature has the same transformation law as the frequency:

$$T_b = \delta T_b^* \quad (2)$$

The observed flux from a point source is

$$S_\nu = \delta^3 S_\nu^* \quad (3)$$

while for a jet the exponent is 2, and in general the exponent can be between 2 and 3 (Lind & Blandford 1985).

If a source component has proper motion μ then it has an apparent transverse speed $\beta_{\text{app}} = \mu D(1+z)/c$, where D is the metric distance to the source. In terms of the source geometry,

$$\beta_{\text{app}} = \frac{\beta \sin \theta}{1 - \beta \cos \theta} \quad (4)$$

Graphs of this relation are in Figure 3.

3 The Observations

3.1 Frequency Shift

Several galactic sources show radio jets that are analogous to those seen in the high-luminosity extragalactic sources. SS 433 contains a jet with radio-bright components which move out from the core, and the jet changes orientation in a way that is consistent with precession. This source also exhibits frequency-shifted Balmer lines that, when tracked over time, show conclusively that the speed of the line-emitting clouds is $\beta = 0.26$ (Margon *et al.* 1980). This value is not relativistic, but it is well above values otherwise associated with stars, including supernovae shock waves. If SS 433, a compact stellar object, can generate a jet with $\beta = 0.26$, then we might expect that an extragalactic object a billion times more luminous can produce a jet that is relativistic.

3.2 Morphology and Doppler Boosting

Early imaging showed that many radio galaxies contain lobes more-or-less symmetrically located across the galaxy, and some objects also contain a bright point source at the center. A good deal of speculation went into the question of how these lobes were formed and energized. They were hundreds or even thousands of kiloparsecs from the center, but their synchrotron lifetimes were only a million years. If they were ejected from the galaxy it must have been at relativistic speed, otherwise there would be a lifetime problem. Alternately, there might be some kind of continuous beams that kept the lobes energized (eg Ryle and Longair 1967).

VLA images then showed that the beams did exist, and that there could be continuous feeding of the lobes. However, in most cases the beams were strongly asymmetric; one side typically was much stronger than the other. Another clue came from VLBI high-resolution studies. Many compact sources were linear but strongly non-symmetric; a bright “core” was at one end of a jet that had a spectral gradient such that the core had the flattest spectrum. See K04 for many examples. An important discovery was that the inner jet nearly always pointed in the direction of the stronger of the two outer jets. How could there be one-sided inner structure with two-sided outer structure? Most astronomers accepted the idea that the jets contained relativistic beams, and Doppler boosting enhanced the forward beam relative to the backward beam.

In 1987 the ‘‘Laing-Garrington effect’’ was discovered (Garrington *et al.* 1988); this was essentially regarded as a proof of the relativity hypothesis. The two outer radio lobes of a radio source typically have different amounts of Faraday rotation, and the lobe with the weaker Faraday effect is nearly always on the jet side. It must be in front, because on average its radiation goes through less plasma than for the one in back, the non-jet lobe. The visible jet then is the one in front, and the only convincing reason that has been offered for this is Doppler boosting.

The front-to-back ratio of the jets, r , is typically greater than 10. This does not call for a very high value of γ , although 3C 273 is exceptionally one-sided, with $r > 5500$ (Davis *et al.* 1985). The compact inner jets often have $r =$ several thousand, which requires $\delta \geq 7$; i.e. $\gamma \geq 3.5$ and $\theta \leq 8.2^\circ$. However, these are the extreme values of γ and θ , and more likely values are $\gamma \sim 7$ and $\theta \sim 6^\circ$. These calculations assume that the jet and counterjet have the same intrinsic luminosity.

Note that the measured high values of r imply small values of θ . *The strongly one-sided objects must be aimed close to the LOS.* What of the mis-directed ones, those more numerous objects not close to the LOS? They are not Doppler-boosted; and in fact most will be deboosted and hence weak. The mis-directed objects are generally thought to be radio galaxies, and indeed these typically have weak cores (Urry & Padovani 1995). The strong, compact, one-sided, flat-spectrum sources often also show superluminal motion, which also requires an orientation close to the LOS. (see §3.6). Given the number of sources that are known to be highly aligned with the LOS, the parent population is likely to be very large (Lister & Marscher 1997). This topic, however, is beyond the scope of this review.

3.3 Interferometric Brightness Temperature

A relativistic plasma will produce synchrotron radiation at radio wavelengths and also X-rays, from the inverse-Compton process. For reasonable values of the magnetic field the maximum intrinsic temperature that the plasma can have, if it is in dynamic equilibrium, is $T_o \sim 10^{12}$ K, because at a higher temperature second order scattering becomes important and rapidly quenches the plasma (Kellermann & Pauliny-Toth 1969). Somewhat similar arguments have been made by Singal (1986) and by Sincell & Krolik (1994) who derive 3×10^{11} K and 2×10^{11} K, respectively, as upper limits. However, Readhead (1994) has argued that because at 10^{12} K the magnetic and kinetic energies in the plasma are very far out of balance, a lower equilibrium temperature, $T_{eq} \sim 5 \times 10^{10}$ K, is more likely to be found.

Measurements made with VLBI show that the temperature can be higher than these values. Figure 1a shows the distribution of T_b measured with the VLBA at 15 GHz (Zensus *et al.* 2002), and Figure 1b shows the distribution measured with the space VLBI program VSOP at 5 MHz (Hirabayashi *et al.* 2000). For both the VLBA and VSOP results, some of the measured values are lower limits. The two distributions are similar and show that some sources have T_b an order of magnitude and more above the SSC and other limits and estimates for T_b described above. Theoretical ways of exceeding the limits have been proposed, including a

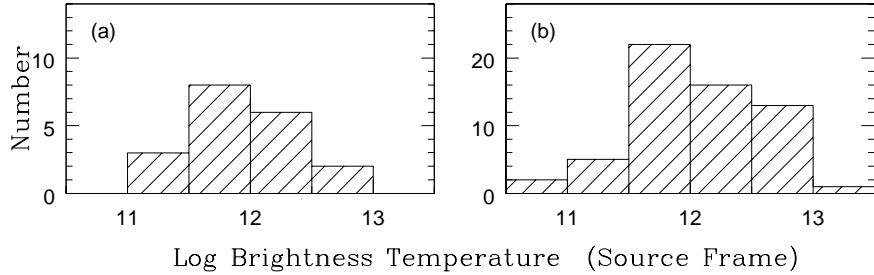


Fig. 1. Distributions of interferometric brightness temperature (a) measured with the VLBA at 15 GHz, $N=19$ (Zensus *et al.* 2002), and (b) measured with VSOP at 5 GHz, $N=59$ (Hirabayashi *et al.* 2000). Note the different vertical scales in (a) and (b).

non-equilibrium plasma (Slysh 1992), and coherent radiation processes (Benford and Lesch 1998). However, we prefer (with most others) to invoke Eq (2) and explain the discrepancy with relativistic motion. We expect that most sources will have $T_o \sim 10^{11}$ K in accord with the estimates of Readhead and others, although we also think there might be a distribution of T_o with a small number of sources approaching 10^{12} . In any event, it is clear that many sources must contain relativistic beams with $\delta = 5 - 10$ and more.

Note that this discussion and the one based on morphology are independent and complementary. They both require Doppler factors up to ~ 10 .

3.4 Variability Brightness Temperature

3.4.1 Intrinsic Variability

Many AGN show rapid variability, with time scale τ as short as a few weeks. With the assumption that τ is limited by the light-crossing time, and with the aid of a model, τ can be turned into an angular diameter. The “variability brightness temperature” T_{var} can then be found from the flux in the outburst. However, Eq (2) is not valid for converting these T_{var} to intrinsic values, T_o , because the transformation of τ introduces another factor of δ , and τ enters twice in calculating the solid angle. Hence, in this case (2) is replaced with

$$T_{\text{var}} = \delta^3 T_o, \quad (5)$$

where T_o is the intrinsic temperature in the plasma. With the assumption of a particular value for T_o , Eq (5) can be used to calculate δ_{var} ; the cube root makes the estimate of δ_{var} somewhat insensitive to the model used in deriving the angular size. Lähteenmäki & Valtaoja (1999) have used their flux monitoring data at 22 and 37 GHz to calculate T_{var} and δ_{var} , for $T_o = 5 \times 10^{10}$ K. Their histogram of δ_{var} is in Figure 2. Their values have been converted to the cosmology we use in this paper, $H_o = 70 \text{ km sec}^{-1} \text{ Mpc}^{-1}$, $\Omega_m = 0.3$, $\Omega_\Lambda = 0.7$. The distribution of δ_{var}

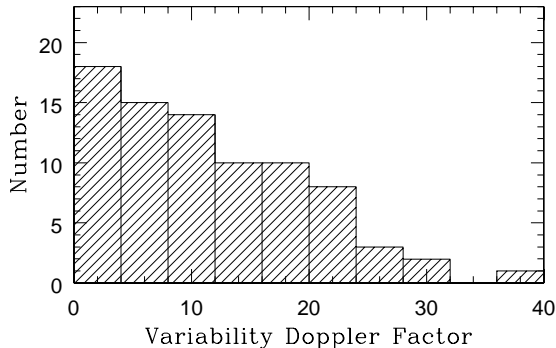


Fig. 2. Distribution of Variability Doppler Factor from Lähteenmäki and Valtaoja (1999), with their cosmology corrected to the values used in this paper. $N=81$

decreases steadily with δ_{var} up to $\delta_{\text{var}} \sim 30$. The model used in these calculations is an optically thick sphere of radius $c\tau$.

If the interferometric data in Figure 1 are converted to δ with the same intrinsic temperature as used for the variability, $T_o = 5 \times 10^{10}$ K, the δ are larger than the ones in Figure 2, and a higher temperature, around $T_o = 10^{11}$ K, is needed to bring them into rough agreement. A detailed comparison cannot be made because the selection criteria for the two data sets are very different; and also because the interferometric data contain a number of lower limits on T_b .

3.4.2 Interstellar Scintillations

Some compact sources show rapid variability due to the passage of the Earth through the irregular diffraction pattern produced by the interstellar medium. This interstellar scintillation can be as fast as a few hours, giving intraday variability, or IDV. Scattering theory gives an estimate of the distance to the screen, and the angular size of the background source. Thus the brightness temperature can be estimated; the method is analogous to VLBI, but with a longer baseline. Analysis of the IDV cases shows that the screen distance is only 10s of pc, and the angular scale is 10s of micro-arcsec (Dennett-Thorpe & de Bruyn 2000). The best-determined case appears to be PKS 0405–385 (Rickett *et al.* 2002), which has $T_b \sim 2 \times 10^{13}$, and $\delta \sim 75$ (for $T_o = 3 \times 10^{11}$, the value used by Rickett *et al.*). The value $\delta \sim 75$, while high, is not unprecedented, because the generally-accepted theory for γ -ray bursts requires jets with $\delta \sim 100$ or more. There are many AGN jets with δ up to about 30, (Fig 2) and a few with δ near 100, but none have been found in-between. Lähteenmäki & Valtaoja (1999) state that, if there were sources with variability time scale $\tau \sim 1$ week at 22 and 37 GHz, they would have

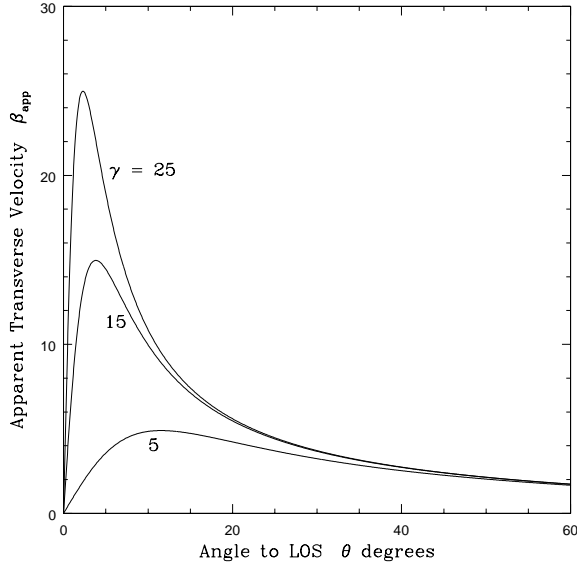


Fig. 3. Apparent transverse velocity β_{app} vs θ , the angle to the line-of-sight. Note that every $\beta_{\text{app}} > 1$ has a maximum possible angle, $\sin \theta_{\text{max}} = 2\beta_{\text{app}}/(1 + \beta_{\text{app}}^2)$ and a minimum Lorentz factor $\gamma_{\text{min}} = (\beta_{\text{app}}^2 + 1)^{1/2}$

been found. However, in view of the selection biases in all these studies, we think it premature to generalize these statistics.

3.5 Inverse-Compton X-rays

A synchrotron source in dynamic equilibrium must radiate X-rays via the inverse-Compton process, but in some cases the measured X-rays are much lower than the value expected from the radio flux density. The accepted explanation for this is relativistic motion, and δ can be estimated if the appropriate radio and X-ray measurements are made (Marscher 1983). The calculation is strongly dependent on the radio diameter, which has to be measured with VLBI. Thus this method is closely allied to the VLBI temperature method (§3.3). The X-rays should be measured simultaneously with the radio, and the radio observations should be made at the peak of the synchrotron spectrum. These conditions are seldom met. Nevertheless, calculations made from literature surveys (eg Ghisellini *et al.* 1993) show that many flat-spectrum sources appear to require $\delta \sim 5 - 10$. Bloom *et al.* (1999), however, show that the errors typically are fairly large, and only a few of the sources in their sample actually require $\delta > 1$. The best case appears to be 3C 345; Unwin *et al.* (1994, 1997) show that in this source δ increases from ~ 5 to ≥ 10 as the radiating component moves out from the core. (These

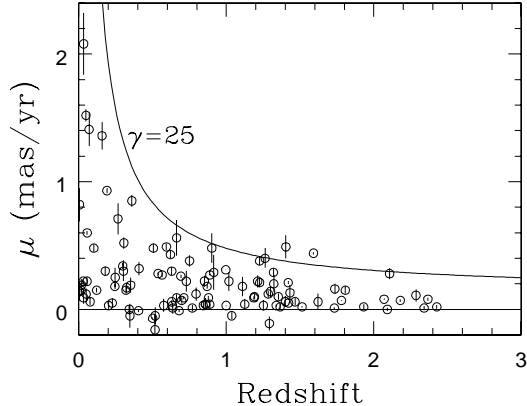


Fig. 4. Proper motion vs redshift (μz diagram) for the fastest “Excellent” or “Good” component for 110 sources in the 15-GHz VLBA survey. The line $\gamma = 25$ is the locus of points where the minimum value of γ is 25; a source on the line can have a higher, but not a lower, value of γ .

values become somewhat larger if the the cosmology used in this review is used.)

3.6 Superluminal Motion

A local observer sees the radiation from a relativistic jet contracted in time, provided $\delta > 1$, and the *apparent* transverse speed, β_{app} , is greater than the speed of light, in some range of θ (Eq. 4). Figure 3 shows β_{app} vs θ for several values of γ ; for $\gamma^2 \gg 1$, β_{app} is a maximum at $\theta \approx 1/\gamma$, and $\beta_{\text{app,max}} \approx \gamma$. Conversely, for a given β_{app} , we have $\gamma_{\text{min}} \approx \beta_{\text{app}}$.

Early VLBI observations showed a number of sources that displayed this superluminal effect (Vermeulen & Cohen 1994). More recently, systematic large-scale surveys have produced more than 100 well-defined superluminal sources. In this section we show some results from a survey on the VLBA, and then discuss alternatives to the relativistic beam for explaining the observations.

Figure 4 shows the μz diagram for the fastest components that are rated E (excellent) or G (good) for 110 sources in the 15-GHz VLBA survey (K04). The solid line, marked $\gamma = 25$, shows the points (μ, z) for which $\gamma \geq 25$. Hence, the points close to the line have $\gamma \approx 25$ or greater, and sources below the line can have correspondingly lower values of γ . This plot shows directly that the measured patterns must be moving relativistically. Figure 5 shows the histogram of β_{app} for the sources in Figure 4. This also is a histogram for γ_{min} .

We note that the fastest component found in even a rather small sample of beamed sources with constant γ will have β_{app} which closely approaches γ (Vermeulen & Cohen 1994). Hence, we take $\gamma_{\text{max}} = 25$ in our later discussions.

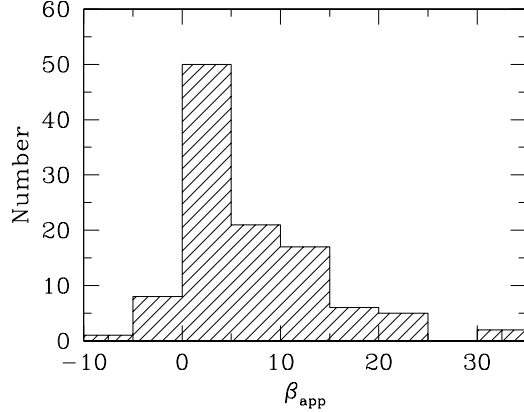


Fig. 5. Histogram of the apparent transverse velocity, β_{app} , for the 110 sources in Figure 4. The median value of β_{app} is 4.2. This also is a histogram of the minimum possible value of γ .

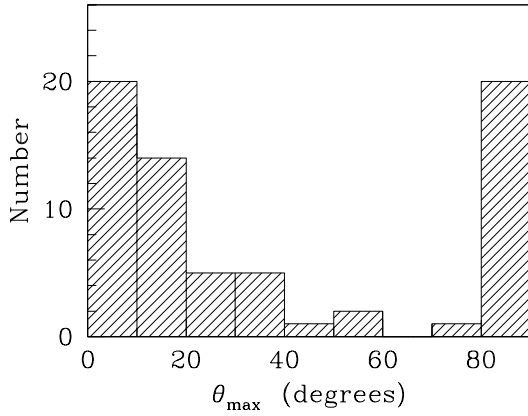


Fig. 6. Histogram of θ_{max} , the maximum possible angle to the LOS, for the 68 sources in Figure 5 that have $S > 1.5$ Jy at 15 GHz. The peak near $\theta_{\text{max}} = 90^\circ$ consists of sources with low or non-significant values of β_{app} which do not constrain the angle.

In reality the value could be somewhat larger, but not smaller.

Any $\beta_{\text{app}} > 1$ has a corresponding maximum possible θ , $\sin \theta_{\text{max}} = 2\beta_{\text{app}} / (1 + \beta_{\text{app}}^2)$ (see Figure 3). The histogram of θ_{max} for the 68 sources with $S > 1.5$ Jy is in Figure 6. We picked this flux density cutoff because it is the limit of the original selection, and the weaker sources probably introduce a serious bias. These 68 sources, roughly speaking, approximate a flux-limited sample. In plotting

this histogram, we set every source with $\beta_{\text{app}} < 2\sigma$ or $\beta_{\text{app}} < 1$ to 90° ; this is responsible for the peak at 90° .

In fact, θ_{max} is highly unlikely to be the actual value of θ for a beamed source. It can be shown that the most probable viewing angle, θ_p , for a source picked on the basis of its flux density from a randomly-oriented beamed population, is about $1/(2\gamma)$ (Lister & Marscher 1997). Since the minimum γ is approximately β_{app} , a rough upper limit to θ_p is $\theta_{\text{max}}/4$. We conclude that the histogram in Figure 6 is unlikely to be representative of the real values of θ ; a more probable distribution would be more peaked at small angles.

Lister and Marscher (1997) show some plots of the distribution of β_{app} and θ from Monte-Carlo simulations of observing a complete well-defined sample of relativistically boosted jets. We have begun to observe such a sample, in a continuation of the 15 GHz VLBA survey called the MOJAVE project (Lister 2003).

3.6.1 Pattern Speed vs Beam Speed

It is usually assumed that the speed measured for the moving pattern is also the speed of the beam, but this often may be wrong (Lind & Blandford 1985). Shocks will exist in the jet, and in some cases the moving blobs will be compressions due to the shocks (Hughes *et al.* 1985). In these cases the pattern speed can be different from the underlying flow velocity. As an extreme case, consider a standing shock wave set up at a bend in the jet; the measured speed (zero) gives no information on the actual flow velocity. Another possibility is that a beam contains two components, a narrow fast spine and a slower sheath. In this case the observed pattern speed might be a combination of the two speeds, although we might see only the spine, because its Doppler boosting will be higher. Other effects, including bending of the beam and evolution in the moving component, can also give erroneous speeds. Nevertheless, in most cases the measured pattern velocity should be similar to the actual beam speed, because the speeds are roughly compatible with other relativity indicators. (See §4.4).

3.6.2 Alternatives to the Relativistic Beam Model

Relativistic beams are generally accepted as the explanation for superluminal motion, but alternatives have been suggested and are still occasionally referred to. These can be grouped into two main categories.

1. Random

Among the 110 sources of the 15-GHz survey, nearly all show expansion or zero velocity. The two sources with a statistically significant (2σ) negative velocity can be reasonably explained with outward helical motion or with a bent jet, as an alternative to contraction. Further, in most cases the motions are along a line, and the expansions can persist for up to a decade in distance from the core. In the two-sided source NGC 1052 (Vermeulen 2003), the speeds are similar on the two sides. These motions are not random.

2. Non-beaming models

The light-echo model (Lynden-Bell 1977) works for supernova remnants but not for jets in AGN, because the predicted distribution of velocities does not match the data. The same problem arises for echoes in a dipole magnetic field (Bahcall & Milgrom 1980). Ekers & Liang (1990) produced an ingenious model of a relativistic excitation wave in a jet, where the radiating material is stationary; *i.e.* it is not swept up by the wave. This suffers from the same problem with the distribution of velocities.

These models do not have relativistic motion of the radiating material, so there is no Doppler favoritism. The selected sources must be oriented randomly relative to the LOS. On the other hand, the distribution in Figure 6, based only on the observed values of β_{app} and without explicitly or implicitly assuming Doppler boosting, shows that the orientations are not random, which would give a $\sin\theta$ distribution.

This result was quantified by Cohen (1990) with an analysis of the 12 strongest sources that were then known. Each source has a solid angle associated with θ_{max} that can be compared with 2π , the total available, in a manner analogous to a V/V_m calculation. The result was that the probability that the objects were drawn from a randomly oriented parent population was small unless the Hubble constant was well above any reasonable value. This calculation can now be repeated with a much better and larger sample, and with a current value for H_0 . The result for the fastest component that is rated E or G, for the 53 quasars that have $S(15) > 1.5$ Jy (the original limit of the 15-GHz survey), is that the probability that they were drawn from a randomly oriented parent population is $p < 6 \times 10^{-6}$. This is a strongly biased estimate because (a) a distribution based on a more probable angle, rather than the maximum angle, would have a smaller probability, and (b) every source with $\beta_{\text{app}} < 2\sigma$ or $\beta_{\text{app}} < 1$ was set to 90 degrees. Thus the estimate for p is conservative, and we conclude that the quasars are not oriented at random, but rather are preferentially close to the LOS. The models without Doppler favoritism are not viable.

An exception to this conclusion could arise if there were obscuration near the equatorial plane, so that small values of θ would be favored. However, we do not see how this could come about. The dust clouds invoked for optical obscuration are transparent at radio wavelengths, and free-free absorption at 15 GHz would require unreasonable densities and masses of plasma.

4 Self-Consistency

The brightness temperature of a source can be determined with interferometry (T_b) and also with flux density variations (T_{var}). Comparisons of the two measures can help determine if the various assumptions underlying these determinations are valid. If T_b and T_{var} are measured then the Doppler factor δ and the intrinsic temperature (T_o) can be calculated with Equations 2 and 5. Lähteenmäki *et al.* (1999a) have done this for several sets of sources, and found that most of the T_o have a range around 10^{11} K. This is rather lower than the SSC limit but close to the other values discussed in §3.3. This suggests that, although the detailed

variability model commonly used is not too realistic, the results none-the-less should have some reliability, and the different measurements pertain to the same relativistic plasma. As discussed in §3.4.1, the sets of δ found by the two methods are in rough agreement with $T_o = 10^{11}$.

Now we consider the relation between the variability Doppler factor δ_{var} and the apparent transverse speed β_{app} , and assume that the same plasma motion affects both phenomena, through the shrinkage of the time scale by the forward relativistic motion. They should be closely connected, but note that high δ_{var} can go with low β_{app} , when $\theta < 1/\gamma$. If δ_{var} and β_{app} are known, we can calculate γ and θ from Eqs 1 and 4, but there is ambiguity because an assumed value of T_o is required for δ_{var} . We test the paradigm by calculating δ_{var} with several values of T_o , and comparing the resulting distribution of points $(\beta_{\text{app}}, \delta_{\text{var}})$ with a Monte-Carlo simulation. This should show whether or not δ_{var} and β_{app} could be related to each other through Eqs 1 and 4, and it might suggest an optimum value for T_o .

The simulation is of the type described by Lister and Marscher (1997). It uses a set of beamed sources that are uniformly distributed in space and isotropically distributed in angle, and have power law distributions of luminosity and Lorentz factor. For the simulation shown here we use power law indices of -2.0 and -1.5, respectively. The calculation draws sources at random and counts those that are above a flux limit.

Figure 7 shows β_{app} plotted against δ_{var} for the 49 sources that have both an “excellent” or “good” value of β_{app} (K04) and a value of δ_{var} from the 22 and 37 GHz variability studies of Lähteenmäki & Valtaoja (1999). We have eliminated five sources with speed consistent with zero and located at a sharp bend in the jet, because we assume that they are connected to stationary shock waves and are not indicative of the motion. The Monte-Carlo simulation is in the top left panel; the other panels represent the observations with δ_{var} calculated with different values of T_o . These plots are discussed further in Cohen *et al.* (2003). The solid lines in Figure 7 represent $\gamma = 25$. A sample of sources with a distribution of γ with $\gamma_{\text{max}} = 25$ will be entirely below the line. We used $\gamma = 25$ following the discussion of Figure 4, and it appears to provide a reasonable envelope.

The probability of finding a beamed source selected on the basis of flux density is maximized well inside the $1/\gamma$ cone (Vermeulen & Cohen 1994); and 72% of the sources in the simulation are indeed inside the cone. In Figures 7b,c,d the fractions are 86%, 71%, and 63%, respectively; and on this basis we would select (c) as providing the best fit to the simulation. But the detailed distribution also suggests that (c) is preferable to (b) or (d), In (b) there is a cluster of points outside the $\gamma = 25$ circle including one at $\delta_{\text{var}} = 70$; however it is hard to judge the importance of this because the errors on δ_{var} are large and not well-understood. The effect becomes exaggerated if T_o is reduced below 1×10^{10} . In (d) the points appear to be clustered rather far to the left, and this is exaggerated if the temperature is raised. The result is that the speeds measured with the VLBA are consistent with the variability Doppler factors provided that the intrinsic temperature is roughly 2×10^{10} K.

The number of points is small and the errors are large, but in Figure 7c,

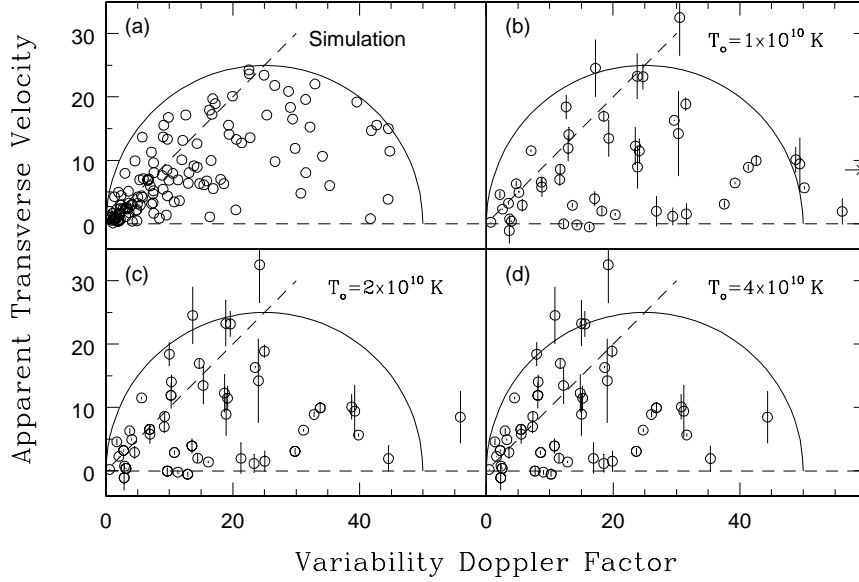


Fig. 7. Simulated and measured values of $(\beta_{\text{app}}, \delta_{\text{var}})$. (a) Simulated flux-limited sample ($N=133$) of beamed sources having $\gamma_{\text{max}} = 25$. The solid line is the locus of points for $\gamma = 25$; the dashed line $\beta_{\text{app}} = \delta_{\text{var}}$ marks the “ $1/\gamma$ cone” around the LOS (see text). (b) The points $(\beta_{\text{app}}, \delta_{\text{var}})$ for the fastest component of the sources having both a β_{app} value from the 15 GHz VLBA survey (K04), and a δ_{var} value from variability studies at 22 and 37 GHz Lähteenmäki & Valtaoja (1999) ($N=49$). The δ_{var} are calculated with intrinsic temperature $T_o = 1 \times 10^{10}$ K. (c) as in (b) with $T_o = 2 \times 10^{10}$ K. (d) as in (b) with $T_o = 4 \times 10^{10}$ K.

for $T_o = 2 \times 10^{10}$ K, the distribution is perhaps matched to the simulation. Cohen *et al.* (2003) discuss the fit. $T_o = 2 \times 10^{10}$ K can be taken as a rough value of the intrinsic temperature. In fact there surely is a distribution of T_o , but there are not enough data to study that.

Figure 8 shows the distribution of γ calculated from the $(\beta_{\text{app}}, \delta_{\text{var}})$ points, with $T_o = 2 \times 10^{10}$ K. Four sources have formally negative values of β_{app} , and in Figure 8 they are plotted as upper limits at the 2σ position. The values above $\gamma = 25$ can be seen above the line in Figure 7. Two of them are within 2σ of $\gamma = 25$, and the third, like all the points, has an unknown error connected with the variability Doppler factor.

The value $T_o \sim 2 \times 10^{10}$ K from the $(\beta_{\text{app}}, \delta_{\text{var}})$ distribution is rather different from the value $T_o \sim 10^{11}$ K from the comparison of interferometer and variability Doppler factors. However, these agree within an order of magnitude and perhaps this is a success, given the many assumptions going into the analyses, and the

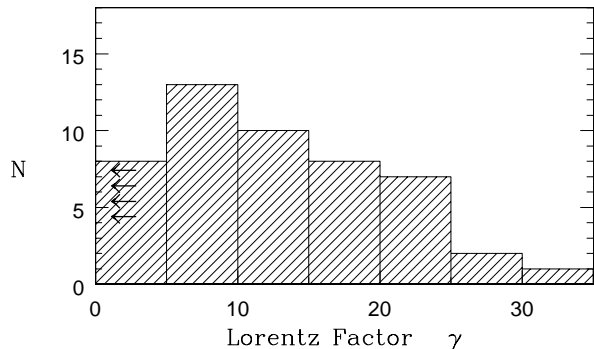


Fig. 8. Histogram of Lorentz factor calculated from δ_{var} and β_{app} with $T_o = 2 \times 10^{10}$ K. Arrows indicate upper limits.

large observational errors.

5 Conclusions

We have described five independent sets of radio phenomena which show that there is relativistic motion in the compact jets of AGN. These are the observations of morphology, interferometry, intrinsic variability, interstellar scintillations, and superluminal motion. X-ray measurements provide further confirmation, although these results are dependent on the VLBI measurements from which the brightness temperatures are determined. Each of these phenomena has a theoretical difficulty which is readily alleviated by assuming that there is bulk relativistic motion towards the observer. The morphology, interferometry, interstellar scintillations, and the X-ray method are independent of redshift and hence of cosmology. Interpretations based on intrinsic variability and on internal proper motion, however, require a knowledge of the distance to the source. The variability methods, and the interferometry method, require an assumption of an intrinsic temperature in the synchrotron cloud. The distribution of δ peaks at low values and decreases to $\delta \sim 30$. The Lorentz factor γ is a more fundamental quantity than δ , but is harder to estimate. Values estimated for γ range up to 34.

A comparison of β_{app} and δ_{var} shows that the superluminal speeds and the variability Doppler factors are roughly consistent with the standard relativistic motion paradigm, provided the intrinsic temperature in the synchrotron clouds is $\sim 2 \times 10^{10}$ K. This value is below the various theoretical upper limits, and is close to Readhead's estimate (1994), based on equipartition between the energy in the particles and that in the magnetic field.

References

- Bahcall, J.N. & Milgrom, M. 1980 ApJ, 236, 24
- Benford, G. & Lesch, H. 1998, MNRAS, 301, 414
- Bloom, S. D. *et al.* 1999, ApJS, 122, 1
- Cohen, M. H. 1990, in Parsec-Scale Radio Jets, ed. J.A. Zensus & T.J. Pearson, (Cambridge: Cambridge University Press), 317
- Cohen, M. H. *et al.*, 2003 in Radio Astronomy at the Fringe, ASP Conference Series No 300, eds JA Zensus *et al.*, 177
- Davis, R.J., Muxlow, T.W.B. & Conway 1985, Nature, 318, 343
- Dennett-Thorpe, J. & de Bruyn, A. G. 2000, ApJ, 529, L65
- Ekers, R.D. & Liang, H. 1990, in Proc. Workshop on Parsec-Scale Jets, (Cambridge: CUP), 333
- Garrington, S.T., Leahy J.P., Conway R.G. & Laing R.A. 1988, Nature, 331, 147
- Ghisellini, G., Padovani, P., Celotti, A. & Maraschi, L. 1993, ApJ, 407, 65
- Hirabayashi, H. *et al.* 2000, PASJ, 52, 997
- Hughes, P. A., Aller, H. D. & Aller M. F. 1985, ApJ, 298, 301
- Hjellming, R. M. & Johnston, K. J. 1981, ApJ, 246, L141
- Kellermann, K.I. & Pauliny-Toth, I.I.K. 1969, ApJ, 155, L71
- Kellermann, K.I. *et al.* 2004, in press; K04
- Lähteenmäki, A., & Valtaoja, E. 1999, ApJ, 521, 493
- Lähteenmäki, A., Valtaoja, E., & Wiik, K. 1999a, ApJ, 511, 112
- Lind, K. R. & Blandford, R. D. 1985, ApJ, 295, 358
- Lynden-Bell D. 1977, Nature, 270, 396
- Lister, M. 2003, in "Future Directions in High Resolution Astronomy: A Celebration of the 10th Anniversary of the VLBA, eds J. Romney *et al.*, in press.
- Lister, M. L. & Marscher, A. P. 1997, ApJ, 476, 572
- Marscher, A.P. 1983, ApJ, 264, 296
- Margon, B., Grandi, S.A. & Downs, R. A. 1980, ApJ, 241, 306
- Readhead, A.C.S. 1994, ApJ, 426, 51
- Rees, M. J. 1966, Nature, 211, 468
- Rickett, B. J., Kedziora-Chudczer, L., & Jauncey, D. L. 2002, ApJ, 581, 103
- Ryle, M. & Longair, M.S. 1962, MN, 136,123
- Sincell, M. W. & Krolik, J. H. 1994, ApJ, 430, 550
- Singal, A. K. 1986, A&A, 155, 242
- Slysh, V.I. 1992, ApJ, 391, 453
- Unwin, S. C., Wehrle, A. E., Urry, C. M., Gilmore, D. M., Barton, E. J., Kjerulf, B. C., Zensus, J. A. & Rabaca, C. R. 1994, ApJ, 432, 103
- Unwin, S. C, Wehrle, A. E., Lobanov, A. P., Madjeski, G. M., Aller, M. F. & Aller, H. D. 1997, ApJ, 480, 596
- Urry, C.M. & Padovani, P. 1995, PASP, 107, 803
- Vermeulen, R.C., Britzen, S., Taylor, G.B., Pearson, T.J., Readhead, A.C.S., Wilkinson, P.N. & Browne, I.W.A. 2003, in Radio Astronomy at the Fringe, ASP Conference Series No 300, eds JA Zensus *et al.*, 43

Vermeulen, R. C. *et al.* 2003, A&A, 401, 113

Vermeulen, R.C. & Cohen, M.H. 1994, ApJ, 430, 467

Zensus, J. A., Ros, E., Kellermann, K. I. Cohen, M. H., Vermeulen, R.C. & Kadler, M.
2002, AJ, 124, 662